ACS NANO

www.acsnano.org

ARTICLE

Molecules, the Ultimate Nanomotor: Linking Chemical Reaction Intermediates to their Molecular Diffusivity

Tian Huang, Bo Li, Huan Wang,* and Steve Granick*

Cite This: *ACS Nano* 2021, 15, 14947−14953

Read Online

ACCESS | Metrics & More | Article Recommendations | Supporting Information

ABSTRACT: The intellectual community focused on nanomotors has recently become interested in extending these concepts to individual molecules. Here, we study a chemical reaction according to whose mechanism some intermediate species should speed up while others slow down in predictable ways, if the nanomotor hypothesis of boosted diffusion holds. Accordingly, we scrutinize the absolute diffusion coefficient (D) during intermediate steps of the catalytic cycle for the CuAAC reaction (copper-catalyzed azide-alkyne cycloaddition click reaction), using proton pulsed field-gradient nuclear magnetic resonance to discriminate between the diffusion of various reaction intermediates. We observe time-dependent diffusion that is enhanced for some intermediate molecular species and depressed for those whose size increases owing to complex formation. These findings point to the failure of the conventional Stokes−Einstein equation to fully explain diffusivity during chemical reaction. Without attempting a firm explanation, this paper highlights aspects of the physics of chemical reactions that are imperfectly understood and presents systematic data that can be used to assess hypotheses.

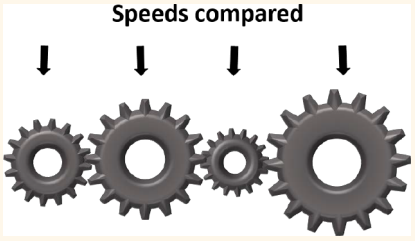

KEYWORDS: *boosted diffusion, NMR, click reaction, intermediates, nanomotor*

The intellectual community focused on nanomotors is motivated by the deep intellectual problems of non-equilibrium nanoscale transport that increasingly offers the promise of practical applications.[1−7] In parallel, it was proposed that enzymes can function as nanomotors, also offering practical applications from using enzymes as materials to direct pumps and other active motion.[8−12] This chain of logic naturally extends to asking if common (non-enzymatic) chemical reactions might show related features of non-equilibrium transport. The idea, proposed long ago by Sen and co-workers,[13] was supported recently by a study from this laboratory of several common chemical reactions.[14] As this concept appears to violate the Stokes−Einstein relation in which diffusivity depends (at fixed temperature and solution viscosity) only on molecular size,[15] there is understandable skepticism.[16] In this paper, we put the hypothesis to direct test by studying a chemical reaction whose known intermediate steps imply predictable changes of molecular diffusivity. If the molecule-as-nanomotor hypothesis holds, then one should observe enhanced diffusion when reactants react chemically, but this should be accompanied by slower diffusion when reactants combine with catalysts to form intermediate reaction complexes of larger size.

Beyond its interesting feature of possessing multiple intermediates whose diffusivity can be discriminated, the reasons we selected the click reaction for study are twofold. The first reason is technical: a wide range of catalyst and reagent concentrations exist that give reactions sufficiently slow to use the pulsed-field NMR technique while satisfying the quasi-steady-state approximation that concentration changes are negligible during the 3−5 min needed to measure each datum.[14,17] The second reason is that click reactions are exceptionally useful and simple to implement with high product yield.[18−24] Our earlier study of molecular diffusivity during the click reaction and several other common chemical reactions was based on two independent experimental methods, a microfluidics design and pulsed field-gradient NMR (PFG-NMR),[14,17] but we did not consider the intermediate reaction steps[23,24] and our analysis involved normalized data rather than its absolute values. Here, inspecting a wider range of reagent stoichiometry, we focus on absolute values of diffusion coefficients and on how the mobility of intermediates in the catalytic cycle correlates with the extent of reaction. As our original publications[14,17] were

Received: June 17, 2021
Published: September 15, 2021

https://doi.org/10.1021/acsnano.1c05168
ACS Nano 2021, 15, 14947−14953

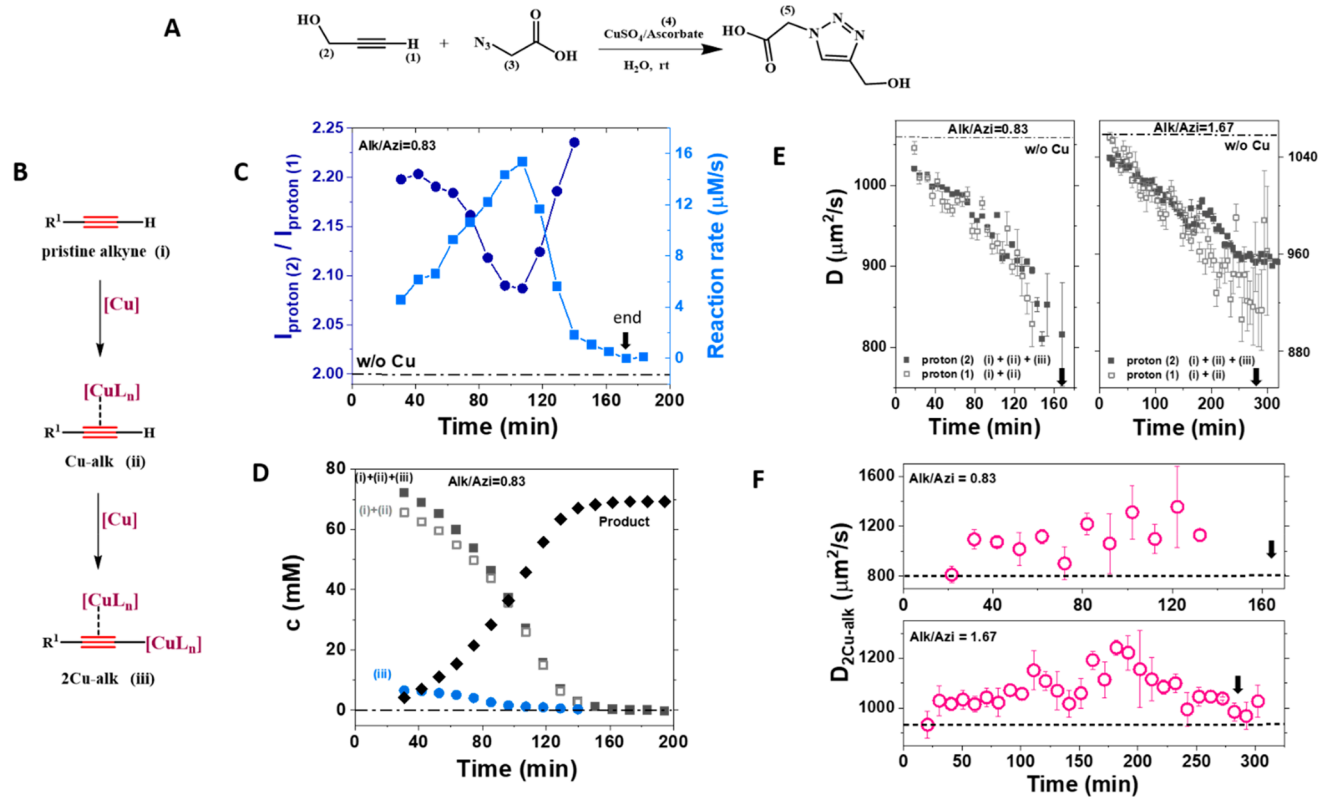

Figure 1. Intermediate steps involving the alkyne reagent, which is the first portion of the click reaction cycle. (A) Net click reaction. The protons measured in this paper by pulsed field-gradient NMR are indicated by numbers (1), (2), (3), and (5); ascorbate peaks (4) were reported on previously.[14] (B) Summary of steps leading from alkyne and Cu(I) catalyst to reactive acetylide complex. (C) Reaction rate (right ordinate) and ratio of peak intensity of protons (2) and (1) (left ordinate) are plotted against time for alkyne:azide = 0.83 (75:90 mM), where reaction rate is calculated from the change rate of the product concentration. (D) Time-dependent total alkyne concentration (species i + ii + iii indicated in panel B); concentration of neat alkyne and Cu-alk (i + ii), concentration of 2Cu-alk (iii), and product concentration are plotted for the same reaction as panel (C). The horizontal dotted line represents the circumstance of no reaction (no added $CuSO_4$). (E) Diffusion coefficients are plotted against time for protons (1) and (2) with alkyne:azide = 0.83 (left panel, 75:90 mM) and alkyne:azide = 1.67 (right panel, 125:75 mM). The horizontal dotted line shows D_i with no reaction (no added $CuSO_4$). (F) Diffusion coefficient of 2Cu-alk for the situations of azide excess (top panel) and alkyne excess (bottom panel) where $D_{2Cu\text{-}alk}$, calculated as described in the text, is averaged from 3 independent experiments with adjacent point averaging to obtain each plotted datum. The dotted line shows the final diffusion coefficient of proton (2) from panel (E). In the data panels, the vertical black arrows show time when the reaction completes.

followed by technical Comments[25,26] about the NMR technique, to which our published Replies explain the reasons for our disagreement,[27,28] those matters are not pursued in this paper. The findings presented here highlight the twin influences of hydrodynamic radius changes, and reaction-induced boosted diffusion.

RESULTS AND DISCUSSION

With proton NMR spectra illustrated in Figure S1, we vary the reactant stoichiometric ratio as this highlights the respective influence of each reactant on diffusion during intermediate steps of the reaction. The net reaction that describes the CuAAC reaction, copper-catalyzed azide-alkyne cycloaddition (Figure 1A), has seen much work devoted in recent years to isolate intermediate products.[29,30]

Alkyne Reagent. At the start, Cu(II) ion is reduced to Cu(I) by ascorbic acid. Alkyne reagent (i) complexes with $[CuL_n]$ to form the intermediate Cu-alk (ii), then subsequently with another $[CuL_n]$ to form a reactive intermediate 2Cu-alk (iii), where the notation L denotes a variety of possible ligands and the literature considers water, ascorbate, and other alkyne molecules to be candidates. The ligand complex is proposed to rearrange rapidly.[31] The terminal alkyne proton is present in (i) and (ii) but not in (iii), which means that NMR can discriminate them. These intermediate steps are summarized schematically in Figure 1B.

The NMR experiments give the intensity change of individual peaks, from which the intensity ratio of proton (2) and proton (1) (Figure 1C) and the time-dependent concentrations of different molecules species (Figure 1D) can be deduced. The NMR measurements also give $D_{proton(1)}$ and $D_{proton(2)}$ (Figure 1E).

Alkyne is the limiting reagent for the stoichiometry alkyne/azide = 0.83, but it is in excess for alkyne/azide = 1.67. Accordingly, all alkyne is converted to 2Cu-alk in the first case, but in the second case, the final state is a mixture of 2Cu-alk and unreacted alkyne. Diffusivity of unreacted alkyne cannot be measured unfortunately, as all of its peaks overlap with those of intermediate steps of the reaction sequence. Interestingly, the intensity ratio of proton (2) and proton (1) is not identically 2 as it would be for the pristine alkyne reagent, but is time-dependent because the 2Cu-alk has no terminal proton (1). Complexation with copper catalyst produces an intermediate of larger molar mass and

https://doi.org/10.1021/acsnano.1c05168
ACS Nano 2021, 15, 14947−14953

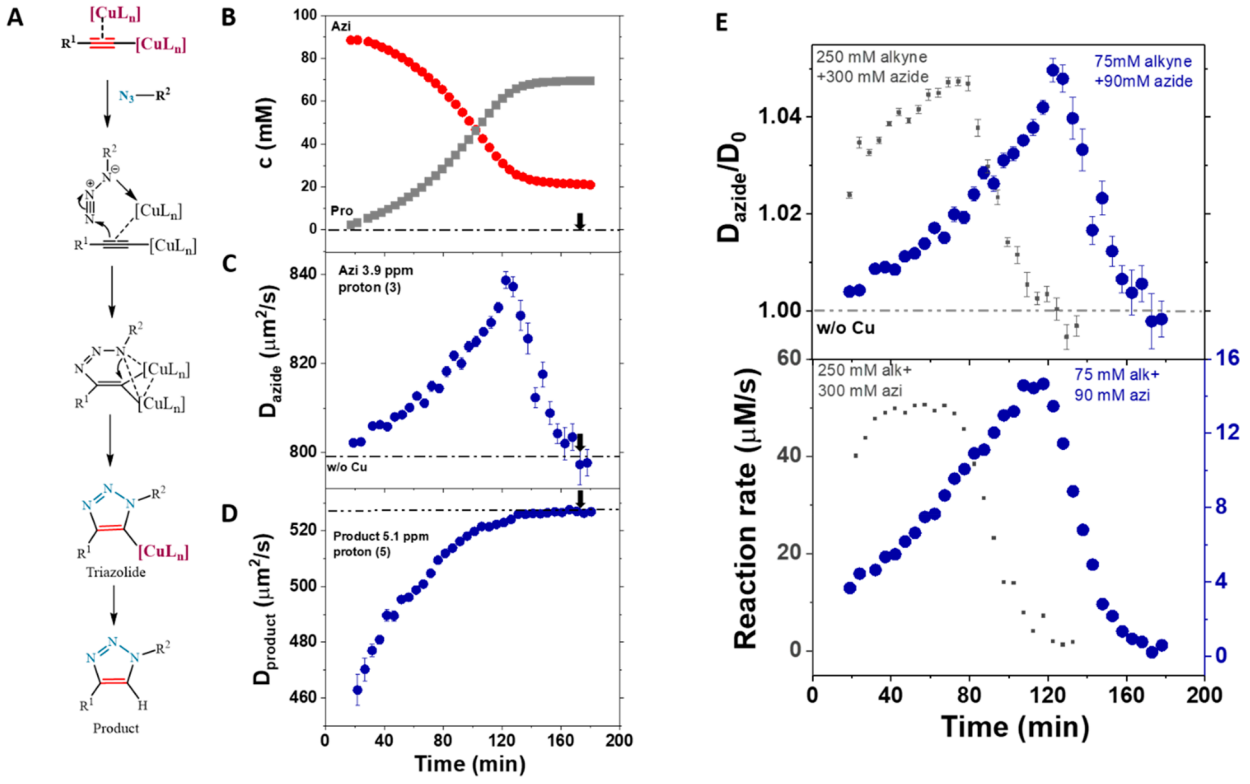

Figure 2. Intermediate steps during which azide reactant adds to copper-alkyne complex, 2Cu-alk. (A) Schematic summary of these reactions steps, ending in product. (B) Time-dependent concentrations of azide and product for alkyne:azide = 0.83, for the same reaction condition as in Figure 1. (C) Time-dependent diffusion coefficient D_{azide} deduced from proton (3). The horizontal dotted line is D_{azide} with no reaction (no added $CuSO_4$). (D) Time-dependent diffusion coefficient $D_{product}$ deduced from proton (5). (E) Comparing boosted diffusion to reaction rate. Top panel: time-dependent ratio, D_{azide}, normalized to its value without added $CuSO_4$, for the same reaction condition as in panel (C) (filled symbols) and for alkyne:azide = 0.83 (250:300 mM; dotted lines) with the latter data taken under the same conditions as in ref 28. Bottom panel: time-dependent reaction rates for the same experiments whose diffusivity is reported in the top panel. Vertical black arrows denote time when the reaction completes.

consequently larger hydrodynamic volume, giving progressively slower diffusion coefficients of alkyne protons (2) (i + ii + iii) and (1) (i + ii).

The molar masses of pristine alkyne (i), Cu-alk (ii), and 2Cu-alk (iii) are 56, 120, and 182 g·mol^{-1}, respectively. From this, the effective radii $R \approx 0.28$, 0.36, and 0.42 nm, respectively, are estimated as the cube root of the molar volume implied by the molar mass and density 0.972 g·cm^{-3}. From the Stokes–Einstein equation, $D = k_BT/6\pi\eta R$, the inverse dependence on R then predicts diffusion coefficients 650 and 560 $\mu m^2 \cdot s^{-1}$ for the Cu-alk and 2Cu-alk complexes, respectively. While these estimates are qualitative as they ignore solvation and approximate the complex molecular shapes as having a single radius, it is evident that there must be a trend toward slower diffusion owing to larger size. In fact, the trend is underestimated by this estimate as it ignores ligand binding, which must further raise the size of the complex. The apparent diffusion coefficient measured during the reaction is considered to be D of each of these species weighted by its molar concentration.

The assumption of independent variables (reasonable because the overall concentration of all species is low) specifies $D_{2Cu\text{-}alk}$. This argument yields $D_{2Cu\text{-}alk}$ even larger than for the pristine alkyne in the absence of reaction (dotted line in Figure 1E) regardless of whether azide or alkyne is in excess (Figure 1F). Scrutinizing this data, one sees that, while $D_{2Cu\text{-}alk}$ appears to increase monotonically when azide is present in excess, there is a maximum when alkyne is in excess. The maximum $D_{2Cu\text{-}alk}$ occurs at roughly the time when the reaction rate is most rapid (Figure S2A). The residual alkyne after reaction completion exists as a form of 2Cu-alk; this complex is believed to experience fast degenerate rearrangement.[31] The baseline value of 2Cu-alk varies according to the reactant stoichiometric ratio (Figure S3A) because the ratio of alkyne and Cu in the 2Cu-alk complex can be different.[32] Consistent with stoichiometric differences, the final diffusion coefficient is faster when the final state contains unreacted alkyne (≈900 $\mu m^2 \cdot s^{-1}$) than when it contains alkyne completed with Cu (≈800 $\mu m^2 \cdot s^{-1}$). This analysis of alkyne diffusion supersedes that in earlier papers from this laboratory in which consequences of complexation with the catalyst were not considered,[14,17] but the qualitative conclusion is unaffected. We conclude that $D_{2Cu\text{-}alk}$ is more rapid than anticipated from its geometrical size.

Azide Reagent. We now consider azide, the reagent that, according to the accepted reaction scheme,[24] adds to the reactive 2Cu-alk complex. This is followed by several short-lived transition states, then a triazolide complex of product with [CuL_n], and finally the pure reaction product. These intermediates are summarized schematically in Figure 2A. We mapped the concentrations of azide and product as a function of time under conditions of azide excess (Figure 2B). In Figure 2C, one sees that D of azide increases during reaction and reverts after reaction to its value in the absence of catalyst. To

https://doi.org/10.1021/acsnano.1c05168
ACS Nano 2021, 15, 14947–14953

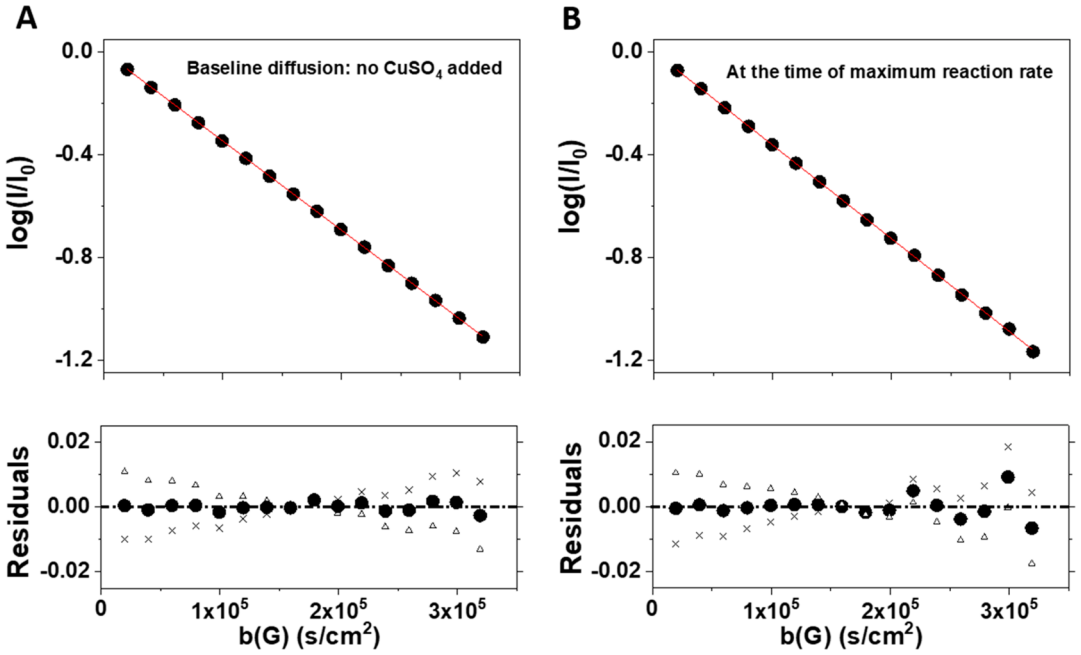

Figure 3. Illustrative fits to the Stejskal−Tanner equation for the azide peak, proton (3), under the condition of excess azide concentration (Alk/Azi = 0.83). Red lines through the data show linear regression under the circumstance of (A) no reaction (no $CuSO_4$ added) and (B) the time of maximum reaction rate. In each panel, the bottom graphs show the residuals to linear regression fit (circles). When these slopes are forced to be 2% larger (crosses) and 2% smaller (triangles) the residuals are systematically worse.

find that the magnitude of boosted diffusion hardly depends on reactant concentration is reminiscent of our earlier finding that it hardly depends on catalyst concentration either.[14]

Figure 2E shows that the peak relative increase of D_{azide} was the same in this experiment as we observed in an early study where the reactant concentration was substantially higher[14,17] (see figure caption). This peak coincides, in both instances, with the time when peak reaction rate was observed.

As a devil's advocate might question the quality of raw data, we call attention to the excellent agreement with the standard model to extract the diffusion coefficient from field gradient NMR data, the Stejskal−Tanner equation.[33] In this model, a plot of NMR peak intensity against calibrated magnetic field gradient on semi-log scales is linear with a slope that specifies the translational diffusion coefficient. For the azide peak of the CuAAC reaction, the illustrations in Figure 3 of linear regression to the data have the correlation coefficient > 0.999. Moreover, residuals to these fits worsen systematically when the slope is forced to be 2% larger or smaller.

Boosted azide diffusion is also measured when alkyne is in stoichiometric excess (Figure S3B). In this case, boosted diffusion persists during the reaction instead of returning to the baseline as shown for azide excess. Because the remaining small amounts of azide are all involved in the reaction near the reaction completion stage, it is reasonable that their diffusion remains boosted. Moreover, $D_{product}$ increases with azide in excess (Figure 2D). This is confirmed with alkyne in stoichiometric excess (Figure S4A).

It would be legitimate to inquire if the azide reactant might aggregate (before reaction) into clusters broken down by chemical reaction. If so, this alternative mechanism could indeed rationalize the maximum we observe (Figure 2) in its diffusion coefficient, but aggregation of this molecule is not expected physically and the diffusion coefficient $D \approx 770\ \mu m^2 \cdot s^{-1}$ calculated with the radius inferred from the molecular density is close to the experimental measurement without reaction, $D \approx 800\ \mu m^2 \cdot s^{-1}$. These arguments do not support the aggregation hypothesis.

Product. An increase of $D_{product}$ is expected from a smaller size when product dissociates from the Cu catalyst. The diffusion coefficient calculated from the hydrodynamic size of the triazole complex, using HyperChem 8.0[34] and HYDRO-PRO[35] software, is 476 $\mu m^2 \cdot s^{-1}$ (Figure S5), which is close to the initial data point. It is intriguing that product dissociation occurs so slowly. The $D_{product}$ saturates roughly after passing the maximum reaction rate (Figure S4B). This may be because protonation of the triazole complex becomes more favorable when 2Cu-alk forms by deprotonation.

CONCLUSION

The underlying molecular mechanism leading to more rapid diffusion is not known, but the experiments presented above are self-consistent. Consistent conclusions emerge not only for the CuAAC reaction that constitutes the subject of this paper but also for other chemical reactions[14] and various catalytic enzymes.[36] Instrumental methods include not only pulsed field gradient NMR[14] but also microfluidics,[14,37,38] fluorescence correlation spectroscopy,[36,39] and dynamic light scattering.[36] Elsewhere, in the Supporting Information to our first publication on the CuAAC reaction,[14] we discussed that temperature, viscosity changes, and convection are not believed to be consistent with this data. The present findings, that diffusion of some intermediates speeds up during reaction while that of others slows down, further support this. Observed in multiple chemical systems using multiple experimental methods, these robust experimental findings present a challenge about the physics of chemical reactions that remains to be understood.

In seeking possible physical mechanisms of why enhanced diffusion may correlate with reaction rate, theoretical models

https://doi.org/10.1021/acsnano.1c05168
ACS Nano 2021, 15, 14947−14953

have begun to appear.[40,41] Upon surveying the literature, we suggest that too little is understood about intramolecular energy flow in which a fast, local component of intramolecular relaxation may be augmented by slower, possibly weaker relaxation.[42,43] Classical Marcus theory[44,45] considers one-dimensional passage between two potential energy wells while all other degrees of freedom are considered, by assumption, to be a random thermal background; it does not deal with the energetics of solvent reorganization, which we conjecture likely to be the crux of this problem. The available spectroscopy experiments focus on using high-energy femtosecond pulses that probe transition states, while slower, lower-energy processes are not measured by the usual ultrafast techniques. However, restructuring of solvent molecules in response to dynamic changes of electric polarization has been noted repeatedly.[46−49] Progress in this area has been impeded by the paucity of experimental and simulation methods capable of exploring slower reorganization than is technically accessible using usual ultrafast laser spectroscopy.

In fact, a growing body of literature considers solvent restructuring during chemical reactions. Orr-Ewing and co-workers have discussed these issues comprehensively.[50−53] In a similar spirit, organic chemists are well aware that reaction rates change according to the solvent.[53−55] Innovative computational and experimental methods continue to be introduced.[56,57] On physical grounds, tentatively, we consider it likely that chemical reactions produce electrified polarization of solvent molecules that solvate the molecules that react, thus providing a mechanism that funnels the rapid (fs) energy release of electronic rearrangement to slower, persistent reorganization of these larger and more diffuse solvation structures. Such reorganization would proceed in multiple steps, corresponding to multiple steps of electronic rearrangement. If this scenario were to hold, one might expect the shapes of solvation shells to wriggle and writhe. Generating propulsion by a kind of swimming, a continuous slow action, could result. Accompanying these processes, the surrounding hydrogen bond network must also adjust to the chemical reaction, and this too may be slow.

Elsewhere, we discussed that local steps of boosted motion accompanied by reorientations from rotational Brownian diffusion would produce a random walk with an effective diffusion coefficient larger than that from just Brownian motion, and we showed plausibility of this argument by comparison with data for catalytic enzymes whose turnover frequency is known.[37,38] Unfortunately, there is no simple way to make a similar comparison for the CuAAC reaction as not enough is yet understood about how to define turnover rate during catalytic cycles.[58] Other factors are also likely to contribute, among them changing solvation layers according to the different lifetimes of the intermediate species of the chemical reaction. Without attempting a firm explanation, this paper highlights systematic data that can be used to assess hypotheses.

METHODS

Our experimental methods are described in the Supporting Information. Proton NMR spectra illustrated in Figure S1 allow multiple protons to be discriminated. The Supporting Information to our first publication on the CuAAC reaction analyzed heat flow from different molecules at different times in the CuAAC reaction using computer simulations and found no support to explain these diffusion data based on a convection hypothesis.[14]

After finding the optimal measurement parameters (relaxation delay time, gradient length, diffusion time), data were collected and analyzed by a home-built code written in IDL (Interactive Data Language).

ASSOCIATED CONTENT

Supporting Information

The Supporting Information is available free of charge at https://pubs.acs.org/doi/10.1021/acsnano.1c05168.

Materials, sample preparations, experimental details, modeling of hydrodynamic radius, NMR spectra (PDF)

AUTHOR INFORMATION

Corresponding Authors

Huan Wang − *College of Chemistry and Molecular Engineering, Peking University, Beijing 100871, People's Republic of China;* orcid.org/0000-0002-2542-936X; Email: wanghuan_ccme@pku.edu.cn

Steve Granick − *Center for Soft and Living Matter, Institute for Basic Science (IBS), Ulsan 44919, South Korea; Departments of Chemistry and Physics, Ulsan National Institute of Science and Technology (UNIST), Ulsan 44919, South Korea;* orcid.org/0000-0003-4775-2202; Email: sgranick@gmail.com

Authors

Tian Huang − *Center for Soft and Living Matter, Institute for Basic Science (IBS), Ulsan 44919, South Korea*

Bo Li − *Center for Soft and Living Matter, Institute for Basic Science (IBS), Ulsan 44919, South Korea*

Complete contact information is available at: https://pubs.acs.org/10.1021/acsnano.1c05168

Notes

The preprint version of this work can be found from the following link: Huang, T.; Li, B.; Wang, H.; Granick, S. Linking Chemical Reaction Intermediates of the Click Reaction to Their Molecular Diffusivity. *ChemRxiv*, **2021**. 10.26434/chemrxiv.14740563.v1 (accessed 2021-06-09).

The authors declare no competing financial interest.

ACKNOWLEDGMENTS

We are indebted to Tsvi Tlusty and Shankar Ghosh for discussions. We thank UCRF (UNIST Central Research Facilities) for supporting the use of the NMR instruments. This study was supported by taxpayers of South Korea through the Institute for Basic Science (project code IBS-R020-D1).

REFERENCES

(1) Sengupta, S.; Dey, K. K.; Muddana, H. S.; Tabouillot, T.; Ibele, M. E.; Butler, P. J.; Sen, A. Enzyme Molecules as Nanomotors. *J. Am. Chem. Soc.* **2013**, *135* (4), 1406−1414.

(2) Paxton, W. F.; Kistler, K. C.; Olmeda, C. C.; Sen, A.; St. Angelo, S. K.; Cao, Y.; Mallouk, T. E.; Lammert, P. E.; Crespi, V. H. Catalytic Nanomotors: Autonomous Movement of Striped Nanorods. *J. Am. Chem. Soc.* **2004**, *126* (41), 13424−13431.

(3) Peng, F.; Tu, Y.; Wilson, D. A. Micro/Nanomotors towards *in Vivo* Application: Cell, Tissue and Biofluid. *Chem. Soc. Rev.* **2017**, *46* (17), 5289−5310.

(4) Sun, J.; Mathesh, M.; Li, W.; Wilson, D. A. Enzyme-Powered Nanomotors with Controlled Size for Biomedical Applications. *ACS Nano* **2019**, *13* (9), 10191−10200.

(5) Venugopalan, P. L.; Esteban-Fernández de Ávila, B.; Pal, M.; Ghosh, A.; Wang, J. Fantastic Voyage of Nanomotors into the Cell. *ACS Nano* **2020**, *14* (8), 9423−9439.
(6) Erbas-Cakmak, S.; Leigh, D. A.; McTernan, C. T.; Nussbaumer, A. L. Artificial Molecular Machines. *Chem. Rev.* **2015**, *115* (18), 10081−10206.
(7) Wilson, M. R.; Solà, J.; Carlone, A.; Goldup, S. M.; Lebrasseur, N.; Leigh, D. A. An Autonomous Chemically Fuelled Small-Molecule Motor. *Nature* **2016**, *534* (7606), 235−240.
(8) Dey, K. K.; Zhao, X.; Tansi, B. M.; Méndez-Ortiz, W. J.; Córdova-Figueroa, U. M.; Golestanian, R.; Sen, A. Micromotors Powered by Enzyme Catalysis. *Nano Lett.* **2015**, *15* (12), 8311−8315.
(9) Ma, X.; Jannasch, A.; Albrecht, U.-R.; Hahn, K.; Miguel-López, A.; Schäffer, E.; Sánchez, S. Enzyme-Powered Hollow Mesoporous Janus Nanomotors. *Nano Lett.* **2015**, *15* (10), 7043−7050.
(10) Patiño, T.; Feiner-Gracia, N.; Arqué, X.; Miguel-López, A.; Jannasch, A.; Stumpp, T.; Schäffer, E.; Albertazzi, L.; Sánchez, S. Influence of Enzyme Quantity and Distribution on the Self-Propulsion of Non-Janus Urease-Powered Micromotors. *J. Am. Chem. Soc.* **2018**, *140* (25), 7896−7903.
(11) Zhao, X.; Gentile, K.; Mohajerani, F.; Sen, A. Powering Motion with Enzymes. *Acc. Chem. Res.* **2018**, *51* (10), 2373−2381.
(12) Ji, Y.; Lin, X.; Wu, Z.; Wu, Y.; Gao, W.; He, Q. Macroscale Chemotaxis from a Swarm of Bacteria-Mimicking Nanoswimmers. *Angew. Chem. Int. Ed.* **2019**, *58* (35), 12200−12205.
(13) Pavlick, R. A.; Dey, K. K.; Sirjoosingh, A.; Benesi, A.; Sen, A. A Catalytically Driven Organometallic Molecular Motor. *Nanoscale* **2013**, *5* (4), 1301−1304.
(14) Wang, H.; Park, M.; Dong, R.; Kim, J.; Cho, Y.-K.; Tlusty, T.; Granick, S. Boosted Molecular Mobility during Common Chemical Reactions. *Science* **2020**, *369* (6503), 537.
(15) Cruickshank Miller, C. The Stokes-Einstein Law for Diffusion in Solution. *Proc. R. Soc. London, Ser. A* **1924**, *106* (740), 724−749.
(16) Zhang, Y.; Hess, H. Chemically-Powered Swimming and Diffusion in the Microscopic World. *Nat. Rev. Chem.* **2021**, *5* (7), 500−510.
(17) Wang, H.; Huang, T.; Granick, S. Using NMR to Test Molecular Mobility during a Chemical Reaction. *J. Phys. Chem. Lett.* **2021**, *12* (9), 2370−2375.
(18) Kolb, H. C.; Finn, M. G.; Sharpless, K. B. Click Chemistry: Diverse Chemical Function from a Few Good Reactions. *Angew. Chem. Int. Ed.* **2001**, *40* (11), 2004−2021.
(19) Meng, G.; Guo, T.; Ma, T.; Zhang, J.; Shen, Y.; Sharpless, K. B.; Dong, J. Modular Click Chemistry Libraries for Functional Screens Using a Diazotizing Reagent. *Nature* **2019**, *574* (7776), 86−89.
(20) Kolb, H. C.; Sharpless, K. B. The Growing Impact of Click Chemistry on Drug Dscovery. *Drug Discov. Today* **2003**, *8* (24), 1128−1137.
(21) Moses, J. E.; Moorhouse, A. D. The Growing Applications of Click Chemistry. *Chem. Soc. Rev.* **2007**, *36* (8), 1249−1262.
(22) Hein, J. E.; Fokin, V. V. Copper-Catalyzed Azide-Alkyne Cycloaddition (CuAAC) and beyond: New Reactivity of Copper(i) Acetylides. *Chem. Soc. Rev.* **2010**, *39* (4), 1302−1315.
(23) Himo, F.; Lovell, T.; Hilgraf, R.; Rostovtsev, V. V.; Noodleman, L.; Sharpless, K. B.; Fokin, V. V. Copper(I)-Catalyzed Synthesis of Azoles. DFT Study Predicts Unprecedented Reactivity and Intermediates. *J. Am. Chem. Soc.* **2005**, *127* (1), 210−216.
(24) Worrell, B. T.; Malik, J. A.; Fokin, V. V. Direct Evidence of a Dinuclear Copper Intermediate in Cu(I)-Catalyzed Azide-Alkyne Cycloadditions. *Science* **2013**, *340* (6131), 457.
(25) Günther, J.-P.; Fillbrook, L. L.; MacDonald, T. S. C.; Majer, G.; Price, W. S.; Fischer, P.; Beves, J. E. Comment on "Boosted Molecular Mobility during Common Chemical Reactions. *Science* **2021**, *371* (6526), No. eabe8322.
(26) Fillbrook, L. L.; Günther, J.-P.; Majer, G.; Price, W. S.; Fischer, P.; Beves, J. E. Comment on "Using NMR to Test Molecular Mobility during a Chemical Reaction. *J. Phys. Chem. Lett.* **2021**, *12* (25), 5932−5937.
(27) Wang, H.; Park, M.; Dong, R.; Kim, J.; Cho, Y.-K.; Tlusty, T.; Granick, S. Response to Comment on "Boosted Molecular Mobility during Common Chemical Reactions. *Science* **2021**, *371* (6526), No. eabe8678.
(28) Huang, T.; Wang, H.; Granick, S. Reply to Comment on "Using NMR to Test Molecular Mobility during a Chemical Reaction. *J. Phys. Chem. Lett.* **2021**, *12* (24), 5744−5747.
(29) Nolte, C.; Mayer, P.; Straub, B. F. Isolation of a Copper(I) Triazolide: A "Click" Intermediate. *Angew. Chem., Int. Ed.* **2007**, *46* (12), 2101−2103.
(30) Jin, L.; Tolentino, D. R.; Melaimi, M.; Bertrand, G. Isolation of Bis(copper) Key Intermediates in Cu-Catalyzed Azide-Alkyne "Click Reaction. *Sci. Adv.* **2015**, *1* (5), No. e1500304.
(31) Makarem, A.; Berg, R.; Rominger, F.; Straub, B. F. A Fluxional Copper Acetylide Cluster in CuAAC Catalysis. *Angew. Chem. Int. Ed.* **2015**, *54* (25), 7431−7435.
(32) Lang, H.; Jakob, A.; Milde, B. Copper(I) Alkyne and Alkynide Complexes. *Organometallics* **2012**, *31* (22), 7661−7693.
(33) Stejskal, E. O.; Tanner, J. E. Spin Diffusion Measurements: Spin Echoes in the Presence of a Time-Dependent Field Gradient. *J. Chem. Phys.* **1965**, *42* (1), 288−292.
(34) Allinger, N. *HyperChem. Release 7 for Windows*; Hypercube, Inc., 2002; Publication HC70-00-01-00.
(35) Ortega, A.; Amorós, D.; García de la Torre, J. Prediction of Hydrodynamic and Other Solution Properties of Rigid Proteins from Atomic- and Residue-Level Models. *Biophys. J.* **2011**, *101* (4), 892−898.
(36) Jee, A.-Y.; Tlusty, T.; Granick, S. Master Curve of Boosted Diffusion for 10 Catalytic Enzymes. *Proc. Natl. Acad. Sci. U. S. A.* **2020**, *117* (47), 29435.
(37) Jee, A.-Y.; Dutta, S.; Cho, Y.-K.; Tlusty, T.; Granick, S. Enzyme Leaps Fuel Antichemotaxis. *Proc. Natl. Acad. Sci. U. S. A.* **2018**, *115* (1), 14.
(38) Jee, A.-Y.; Cho, Y.-K.; Granick, S.; Tlusty, T. Catalytic Enzymes Are Active Matter. *Proc. Natl. Acad. Sci. U. S. A.* **2018**, *115* (46), E10812.
(39) Muddana, H. S.; Sengupta, S.; Mallouk, T. E.; Sen, A.; Butler, P. J. Substrate Catalysis Enhances Single-Enzyme Diffusion. *J. Am. Chem. Soc.* **2010**, *132* (7), 2110−2111.
(40) Tyagi, N.; Cherayil, B. J. Effects of Reactivity on Mobility: Insights from an Exactly Solvable Two-State Model. *J. Stat. Mech.: Theory Exp.* **2021**, *2021* (8), 083204.
(41) Samanta, T.; Sarhangi, S. M.; Matyushov, D. V. Enhanced Molecular Diffusivity through Destructive Interference between Electrostatic and Osmotic Forces. *J. Phys. Chem. Lett.* **2021**, *12* (28), 6648−6653.
(42) Flowers, M. C.; Frey, H. M. Hot Molecule Effects in the Thermal Isomerization of Methylbicyclo[2.1.0]pent-2-enes. *J. Am. Chem. Soc.* **1972**, *94* (24), 8636−8637.
(43) Bragg, A. E.; Cavanagh, M. C.; Schwartz, B. J. Linear Response Breakdown in Solvation Dynamics Induced by Atomic Electron-Transfer Reactions. *Science* **2008**, *321* (5897), 1817.
(44) Gruebele, M.; Wolynes, P. G. Vibrational Energy Flow and Chemical Reactions. *Acc. Chem. Res.* **2004**, *37* (4), 261−267.
(45) Marcus, R. A.; Sutin, N. Electron Transfers in Chemistry and Biology. *Biochim. Biophys. Acta, Rev. Bioenerg.* **1985**, *811* (3), 265−322.
(46) Jimenez, R.; Fleming, G. R.; Kumar, P. V.; Maroncelli, M. Femtosecond Solvation Dynamics of Water. *Nature* **1994**, *369* (6480), 471−473.
(47) Hsu, C.-P.; Song, X.; Marcus, R. A. Time-Dependent Stokes Shift and Its Calculation from Solvent Dielectric Dispersion Data. *J. Phys. Chem. B* **1997**, *101* (14), 2546−2551.
(48) Dinpajooh, M.; Newton, M. D.; Matyushov, D. V. Free Energy Functionals for Polarization Fluctuations: Pekar Factor Revisited. *J. Chem. Phys.* **2017**, *146* (6), 064504.
(49) Meng, X.; Guo, J.; Peng, J.; Chen, J.; Wang, Z.; Shi, J.-R.; Li, X.-Z.; Wang, E.-G.; Jiang, Y. Direct Visualization of Concerted Proton

Tunnelling in a Water Nanocluster. *Nat. Phys.* **2015**, *11* (3), 235−239.
(50) Orr-Ewing, A. J. Perspective: Bimolecular Chemical Reaction Dynamics in Liquids. *J. Chem. Phys.* **2014**, *140* (9), 090901.
(51) Dunning, G. T.; Glowacki, D. R.; Preston, T. J.; Greaves, S. J.; Greetham, G. M.; Clark, I. P.; Towrie, M.; Harvey, J. N.; Orr-Ewing, A. J. Vibrational Relaxation and Microsolvation of DF after F-Atom Reactions in Polar Solvents. *Science* **2015**, *347* (6221), 530.
(52) Orr-Ewing, A. J. Taking the Plunge: Chemical Reaction Dynamics in Liquids. *Chem. Soc. Rev.* **2017**, *46* (24), 7597−7614.
(53) Carpenter, B. K.; Harvey, J. N.; Orr-Ewing, A. J. The Study of Reactive Intermediates in Condensed Phases. *J. Am. Chem. Soc.* **2016**, *138* (14), 4695−4705.
(54) Parker, A. J. Protic-Dipolar Aprotic Solvent Effects on Rates of Bimolecular Reactions. *Chem. Rev.* **1969**, *69* (1), 1−32.
(55) Morris, W.; Lorance, E. D.; Gould, I. R. Understanding the Solvent Contribution to Chemical Reaction Barriers. *J. Phys. Chem. A* **2019**, *123* (49), 10490−10499.
(56) Biasin, E.; Fox, Z. W.; Andersen, A.; Ledbetter, K.; Kjær, K. S.; Alonso-Mori, R.; Carlstad, J. M.; Chollet, M.; Gaynor, J. D.; Glownia, J. M.; Hong, K.; Kroll, T.; Lee, J. H.; Liekhus-Schmaltz, C.; Reinhard, M.; Sokaras, D.; Zhang, Y.; Doumy, G.; March, A. M.; Khalil, M.; et al. Direct Observation of Coherent Femtosecond Solvent Reorganization Coupled to Intramolecular Electron Transfer. *Nat. Chem.* **2021**, *13* (4), 343−349.
(57) Guo, C.; He, X.; Rong, C.; Lu, T.; Liu, S.; Chattaraj, P. K. Local Temperature as a Chemical Reactivity Descriptor. *J. Phys. Chem. Lett.* **2021**, *12* (23), 5623−5630.
(58) Kozuch, S.; Martin, J. M. L. Turning Over" Definitions in Catalytic Cycles. *ACS Catal.* **2012**, *2* (12), 2787−2794.

https://doi.org/10.1021/acsnano.1c05168
ACS Nano 2021, 15, 14947−14953